



Published in final edited form as:

*J Magn Reson.* 2014 December ; 249: 72–79. doi:10.1016/j.jmr.2014.09.020.

## CW Dipolar Broadening EPR Spectroscopy and Mechanically Aligned Bilayers Used to Measure Distance and Relative Orientation between Two TOAC Spin Labels on an Antimicrobial Peptide

Indra D. Sahu<sup>1</sup>, Eric J. Hustedt<sup>2</sup>, Harishchandra Ghimire<sup>1</sup>, Johnson J. Inbaraj<sup>1</sup>, Robert M. McCarrick<sup>1</sup>, and Gary A. Lorigan<sup>1,\*</sup>

<sup>1</sup>Department of Chemistry and Biochemistry, Miami University, Oxford, OH 45056

<sup>2</sup>Department of Molecular Physiology and Biophysics, Vanderbilt University, Nashville, TN 37232

### Abstract

An EPR membrane alignment technique was applied to measure distance and relative orientations between two spin labels on a protein oriented along the surface of the membrane. Previously we demonstrated an EPR membrane alignment technique for measuring distances and relative orientations between two spin labels using a dual TOAC-labeled integral transmembrane peptide (M28 segment of Acetylcholine receptor) as a test system. In this study we further utilized this technique and successfully measured the distance and relative orientations between two spin labels on a membrane peripheral peptide (antimicrobial peptide magainin-2). The TOAC-labeled magainin-2 peptides were mechanically aligned using DMPC lipids on a planar quartz support, and CW-EPR spectra were recorded at specific orientations. Global analysis in combination with rigorous spectral simulation was used to simultaneously analyze data from two different sample orientations for both single- and double-labeled peptides. We measured an internitroxide distance of 15.3 Å from a dual TOAC-labeled magainin-2 peptide at positions 8 and 14 that closely matches with the 13.3 Å distance obtained from a model of the labeled magainin peptide. In addition, the angles determining the relative orientations of the two nitroxides have been determined, and the results compare favorably with molecular modeling. This study demonstrates the utility of the technique for proteins oriented along the surface of the membrane in addition to the previous results for proteins situated within the membrane bilayer.

### Keywords

Dipolar Broadening CW-EPR; Aligned DMPC bilayers; Distance measurement; Antimicrobial peptide; Magainin-2

\*To whom correspondence should be addressed. Telephone: (513) 529-2813, Fax: (513) 529-5715, gary.lorigan@miamioh.edu.

**Publisher's Disclaimer:** This is a PDF file of an unedited manuscript that has been accepted for publication. As a service to our customers we are providing this early version of the manuscript. The manuscript will undergo copyediting, typesetting, and review of the resulting proof before it is published in its final citable form. Please note that during the production process errors may be discovered which could affect the content, and all legal disclaimers that apply to the journal pertain.

**Supporting Information:** Molecular dynamics simulation methods, Figure S1, S2, S3, and S4

## 1. Introduction

In this study, an EPR membrane alignment technique previously shown to be able to measure distances and relative orientations between spin labels on an integral membrane protein is applied to a protein oriented along the surface of the membrane [1]. Membrane-bound proteins play important roles in controlling physiological function in organisms. However, it can often be difficult to obtain the detail structural information needed to determine how these important proteins function. Electron paramagnetic resonance (EPR) spectroscopy in association with site-directed spin labeling (SDSL) can provide unique structural and dynamic information for membrane protein systems [1–7]. Intermediate range distances (8 – 25 Å) can be obtained by measuring line broadening due to dipolar coupling using continuous wave (CW)-EPR [8–10], while longer range distances (20 - 80 Å) can be obtained using the pulsed EPR technique Double Electron Electron Resonance (DEER) [11–16]. Recently, we demonstrated the utility of EPR membrane alignment techniques for measuring both the distance and relative orientation between two TOAC spin labels on the M28 segment of the Acetylcholine receptor, an integral transmembrane peptide [1]. In this study, we successfully applied this approach for the doubly TOAC labeled antimicrobial peptide magainin-2, a membrane peripheral peptide. In general, for dipolar line broadening experiments on randomly dispersed samples, the distances can be estimated by spectral analysis based on Fourier convolution/deconvolution methods [10, 17–19]. Here we used a method of rigorous spectral simulations taking into account both the interspin distance and the relative orientations between the nitroxide spin labels [1, 8, 9, 20, 21].

The EPR membrane alignment technique in this study utilizes a glass cover slip for the support of a lipid and peptide dispersion. To reduce the freedom of movement of the spin labels, the rigid spin label TOAC (2,2,6,6-tetramethyl-piperidine-1-oxyl-4-amino-4-carboxylic acid), which is directly coupled to the protein backbone, was employed. TOAC has been shown to give less disorder in the distance and relative orientation between the two nitroxides without disturbing the structure and function of helices in the case of a soluble and membrane peptide [1, 8]. <sup>15</sup>N solid-state NMR alignment techniques can be used to probe membrane protein/peptide topology [22–26]. However, due to its lower sensitivity and conformational heterogeneity in membrane protein samples, a large amount of purification and tedious sample preparation is needed to obtain high quality NMR results. EPR can provide high quality data with small amount of sample (microgram scale) without utilizing expensive isotopic labels. Anisotropic EPR spectra of aligned samples reveal linewidths that are sharper than powder spectra of randomly dispersed samples, allowing distance and orientation information to be obtained more reliably and accurately when data from two different sample orientations are globally analyzed [1].

Antimicrobial peptides (AMPs) are an important class of peripheral peptides having an increased prevalence within drug-resistant species [27]. AMPs are also promising agents for anticancer therapy [28, 29]. Here, we investigate one of the more potent surface antimicrobial peptides magainin-2. Magainin-2 is known to lie on the membrane surface, roughly perpendicular to the bilayer normal, and serves a critical role for pore formation in bacterial membranes [23]. It has been well investigated for its antiaction on various microorganisms and tumor cells [30–33]. It is a 23-residue peptide, which forms an  $\alpha$ -

helical structure in phospholipid bilayers with a helical tilt of 81° with respect to the membrane normal [5, 34].

The experimental distance and the relative orientations of the TOAC nitroxides were compared with unoriented spectra and molecular modeling studies of dual TOAC-labeled magainin-2 peptide. The results revealed that the relative geometry between TOAC labels can be measured more accurately and precisely when the samples are aligned with respect to the magnetic field. The successful demonstration of the utilization of EPR membrane alignment technique on the membrane peripheral peptide (current study) and integral membrane peptide (previous study) [1] suggests that this EPR membrane alignment technique will become an important biophysical tool to answer pertinent structural questions on membrane associated biological systems.

## 2. Experimental Methods

### Materials

1, 2-Dimyristoyl-sn-glycero-3-phosphocholine (DMPC) pre-dissolved in chloroform was obtained from Avanti Polar Lipids (Alabaster, AL). Fmoc-Arg (Pbf)-Nova Syn TGA resin (0.23 mmol/g), 9-Fluorenylmethyl-oxycarbonyl-O-succinimide (Fmoc-OSu) and all amino acids were purchased from Novabiochem, San Diego, CA. Triisopropylsilane (TIS), anisole, hexafluoro-2-propanol (HFIP), 30% ammonium hydroxide [NH<sub>3</sub> (aq.)], piperidine were purchased from Sigma-Aldrich, St. Louis, MO. 2,2,6,6-Tetramethylpiperidine-1-oxyl-4-carboxylic acid (TOAC) was purchased from Acros Organics, Belgium. Trifluoroacetic acid (TFA), 1-hydroxybenzo-triazole (HOBt), (2-(7-Aza-1H-benzotriazole-1-yl)-1,1,3,3-tetramethyluronium hexafluorophosphate (HATU), diisopropylethylamine (DIEA), N-methyl-pyrrolidone (NMP), and dichloromethane (DCM) were purchased from Applied Biosystems, Foster City, CA. Acetic anhydride (Ac<sub>2</sub>O) and methyl-tert-butyl ether were purchased from Fisher Scientific, Pittsburgh, PA.

### Peptide synthesis and purification

Solid-phase peptide synthesis was carried out on a ABI 433A peptide synthesizer (Applied Biosystems Inc., Foster City, CA) using Fmoc-protection chemistry. The following are the amino acid sequences of the membrane peripheral Magainin-2 peptide used in this study:

<sup>1</sup> GIGKFLHSAKKFGKAFVGEIMN <sup>23</sup> S	wild-type (WT)
<sup>1</sup> GIGKFLH <sup>8</sup> XAKKFGKAFVGEIMN <sup>23</sup> S	singly-labeled TOAC8
<sup>1</sup> GIGKFLHSAKKFG <sup>14</sup> XAFVGEIMN <sup>23</sup> S	singly-labeled TOAC14
<sup>1</sup> GIGKFLH <sup>8</sup> XAKKFG <sup>14</sup> XAFVGEIMN <sup>23</sup> S	doubly-labeled

doubly-labeled where, X represents the location of the TOAC spin label.

The 433A peptide synthesizer connected with a UV-detector (wavelength 301 nm) was used to monitor the removal of the Fmoc-group from the N-terminus of the growing peptide. A modified version of 0.1 mmol Fmoc chemistry protocol in the SynthAssist 2.0 software from

Applied Biosystems was used for peptide synthesis. Software modifications were made to include special functions such as double coupling, increased reaction times, and incorporation of unnatural amino acids in order to facilitate the optimal synthesis of peptides. All amino acids purchased were of the Fmoc-protected and side-chain-protected form to minimize the unnecessary reactions during peptide synthesis. For site-specific TOAC labeling by solid-phase peptide synthesis, the amino terminal of the TOAC was protected with an Fmoc group. The synthesis of Fmoc-TOAC was carried out following standard procedures from the literature [35, 36]. The TOAC-7 labeled magainin peptides were synthesized following the standard protocol published in the literature [1, 5, 37–39]. To optimize the peptide synthesis, the superior coupling agent HATU/HOAt [40] was used for attaching the TOAC spin label and surrounding amino acids (2 preceding the TOAC and 3–4 subsequent) with extended coupling times. This step was necessary to ensure the attachment of the TOAC spin label and to prevent the peptide truncation just after the TOAC attachment due to the low nucleophilicity reaction of the TOAC amino group in a peptide chain [37, 41]. The rest of the amino acids were attached using HBTU/HOBt coupling reagent.

About 150 mg of peptide resin was treated with a cleavage mixture [8.5 mL TFA (trifluoroacetic acid), 0.5 mL TIS (triisopropyl silane), 0.5 mL anisole, and 0.5 mL distilled water] for 3 hours to remove the side chain protecting groups and detach peptides from the resin beads. The peptide mixture was filtered, and the resins were rinsed with TFA and removed. The filtrate was concentrated and precipitated in ice-cold methyl *tert*-butyl ether. The peptides were collected by centrifugation and vacuum dried overnight. The crude peptides were purified on Amersham Pharmacia Biotech AKTA Explorer 10S HPLC system using a reversed phase C-18 semiprep column (Vydac cat. # 218TP1010, 10 $\mu$ m, 10 mm  $\times$ 250 mm). The HPLC solvent system for peptide purification contained H<sub>2</sub>O with 0.1% TFA as solvent A and the mixture of 90% acetonitrile (MeCN), and 10% water with 0.1% TFA as solvent B. The TOAC8 peptide was double purified with a slightly modified solvent system on a reversed phase C-4 semiprep column (Vydac cat. # 214TP1010, 10 $\mu$ m, 10mm  $\times$ 250 mm) to obtain high purity. Since trifluoroacetic acid converts the nitroxide spin label into hydroxylamine form during peptide cleavage and purification, the purified peptides were dissolved in 70:30 n-propanol:water mixture and treated with a few drops of 10% aq. ammonia (pH=9.5) for 3 hours to regenerate the radical signal of the TOAC nitroxide. The purity of the peptides were confirmed by matrix assisted laser desorption ionization time of flight (MALDI-TOF) mass spectrometry to be ~ 95%.

### Sample Preparation

The mechanically aligned glass plate samples were made following the standard procedures described in the literature [1, 5, 42, 43]. Briefly, approximately 75  $\mu$ g of labeled peptide was dissolved in 50  $\mu$ L, 1:1 mixture of TFE and chloroform and mixed with 5 mg of DMPC phospholipid pre-dissolved in chloroform (250  $\mu$ L, conc. 20 mg/mL). The lipid peptide mixture was subjected to a slow stream of N<sub>2</sub>-gas to reduce the final volume to 50–60  $\mu$ L and then 10  $\mu$ L of this peptide lipid mixture was uniformly plated on 5 glass plates (dimension: 5.7  $\times$ 12 mm, Marienfeld GmbH & Co.KG, Germany). The lipids on the glass plates were air-dried for approximately 10 minutes and then vacuum dried overnight in a desiccator. The glass plates were then hydrated with 4  $\mu$ L of purified water and mounted in a

stack. The stacked glass plates were kept for 12 hr in a hydration chamber of saturated ammonium phosphate monobasic solution (temperature 42°C, relative humidity 93%). The next day, the stacked glass plates were covered by double-sided tape and mounted on a glass rod with a flat quartz end and inserted into an EPR cavity to record CW-EPR spectra. Multilamellar vesicles were prepared from the same composition of peptide-lipid mixture in a glass tube (12 × 75 mm) and drying the sample completely in a stream of nitrogen gas followed by overnight drying in vacuum pump desiccators. Subsequently, 100 μL of purified water was added to the tube, and the sample was vortexed constantly. Periodic sample heating was applied by immersing the tube into a hot water bath at 60 °C to achieve complete dissolution of the lipids. The multilamellar vesicles suspension was drawn into a capillary tube, sealed and CW-EPR spectra were recorded in standard quartz EPR tube (Wilmad, 707-SQ-250M).

### EPR Spectroscopy

EPR experiments were performed on a Bruker EMX X-band CW-EPR spectrometer consisting of an ER041xG microwave bridge and ER4119-HS cavity coupled with a BVT 3000 nitrogen gas temperature controller (temperature stability ± 0.2K) at 9.434 GHz microwave frequency, 10 mW microwave power, 100 kHz modulation frequency, and 1.0 G modulation amplitude. EPR spectra were recorded aligning the glass plate samples with the membrane normal,  $\vec{n}$ , either parallel ( $\epsilon = 0^\circ$ ) or perpendicular ( $\epsilon = 90^\circ$ ) to the direction of the static magnetic field,  $B_0$ . A 42-s field sweep scan with sweep-width of 100 G was applied. All EPR spectra were collected at 318 K. At 318 K, DMPC exists in the liquid crystalline phase and the alignment of the DMPC bilayers is optimal [38].

### Analysis of EPR Spectra

All EPR data were analyzed using the methods described previously[1]. A global data analysis program was used to fit all the EPR spectra [1, 8, 9, 20, 44]. This program uses our recently developed algorithms for the non-linear least-squares analysis of multiple data sets utilizing the Levenberg-Marquardt algorithm to find the optimal set of parameters[1]. This approach allows the simultaneous fitting of data sets obtained at two different sample orientations ( $\epsilon = 0^\circ$  and  $\epsilon = 90^\circ$ ). Figure 1 shows all the angles used in this study.

The EPR spectra of randomly-dispersed singly-labeled peptides were analyzed to determine the values of the diagonalized A- and g-tensors for the TOAC label at the two sites. These tensor values were then used as starting values in all subsequent analyses.

For the case of singly-labeled aligned peptides the fit parameters are the angles  $\theta$ ,  $\phi$ ,  $\psi_0$ , and  $\sigma_\psi$  along with A and g components, where the angles  $\theta$  and  $\phi$  determine the orientation of the nitroxide with respect to the helix axis, A is the hyperfine interaction tensor, and g is the g-tensor. For the surface helix used in this study, a previously determined helix tilt ( $\nu = 81^\circ$ ) [5] was used as a fixed parameter during the fit. The rotation of the peptide about the helix axis is determined by  $\psi$ . Better fits to the data presented in this study were obtained when spectra were calculated for a Gaussian distribution of  $\psi$  values centered at  $\psi_0$  with standard deviation  $\sigma_\psi$ . Thus, spectra were generated for  $N_\psi$  values of  $\psi$  and the final result calculated as the sum weighted by the probability of a given  $\psi$  value.

For the case of the doubly-labeled peptides, the values of  $\theta$ ,  $\phi$ ,  $\psi_0$ , and  $\sigma_\psi$  were fixed to those obtained for the singly-labeled peptides at 14th position (nitroxide 1), while the values of the angles  $\alpha$ ,  $\beta$ ,  $\gamma$ ,  $\xi$ , and  $\eta$  together with the interelectron distance  $R$  were varied to optimize the fit to the data, where  $\alpha$ ,  $\beta$ , and  $\gamma$  are three Euler's angles and  $\xi$  and  $\eta$  determine the orientation of  $R$  with respect to nitroxide at 14<sup>th</sup> position. In both cases, the Lorentzian components of the linewidths were allowed to vary independently for the two different sample orientations. A variable fraction,  $f_{\text{iso}}$ , of a non-aligned isotropic component is included in each fit. Confidence intervals for the various fit parameters were obtained by fixing each particular parameter to a linear sequence of values and allowing all of the other fit parameters to vary to find the optimal fit. This determines how  $\chi^2$  varies as a function of a particular parameter and thus gives a measure of the uncertainty in the parameter value.

### Modeling studies of TOAC labeled peptides

The modeling study of magainin-2 peptides was carried out using previously described methods [1]. The NMR structure of the magainin-2 peptide (PDB ID: 2MAG) was used as the starting coordinates for molecular modeling studies [34]. The TOAC spin label was incorporated into the specific sites of the peptide using AMBER94 force field parameters within the MolMol program [1, 45]. The TOAC-labeled magainin peptides were modeled using visual molecular dynamics modeling (VMD) software[46]. From these models, estimates of the angles ( $\theta$ ,  $\phi$ ,  $\xi$ ,  $\eta$ ,  $\alpha$ ,  $\beta$ , and  $\gamma$ ) and interelectron distance ( $R$ ) were obtained for comparison with the experimental results.

All the calculations were performed using a Mathematica [47] script. In order to more directly compare the nitroxide axes in Cartesian space, the results from fitting the EPR data to the model of the doubly-labeled peptide were used to reverse these procedures so that for a given set of  $R$ ,  $\xi$ ,  $\eta$ ,  $\alpha$ ,  $\beta$ , and  $\gamma$  values the corresponding  $x$ -,  $y$ -, and  $z$ -axes of nitroxide 2 (TOAC8) can be calculated relative to nitroxide 1 (TOAC 14).

### Molecular Dynamics Simulation on Wild-type Magainin-2 in DMPC Bilayers

The molecular dynamics simulations on wild-type magainin-2 peptide (PDB ID: 2MAG) in DMPC bilayers and water were performed using NAMD [48] version 2.9 with the CHARMM36 force field [49, 50]. CHARMM-GUI [51] (<http://www.charmm-gui.org>) was used for simulation set up and input generation, and Visual Molecular Dynamics software, VMD [46] version 1.9.1 was used for MD trajectory analysis. The equilibration and minimization was performed under NAMD using the input files generated by CHARM-GUI. The final NAMD production run was collected out to ~ 6 ns following similar simulation conditions described in the literature [52]. The details of the simulation methods are described in the supporting information.

## 3. Results and Discussions

Figure 2 shows the CW-EPR spectra of singly-labeled magainin-2 peptides labeled with TOAC at residue 8 (TOAC8) and residue 14 (TOAC14). The upper panels contain the spectra (black) of the randomly dispersed samples which are well-fit as rigid-limit powder

patterns (red lines) to give the  $g$ - and  $A$ -tensor values (Table 1) used in all subsequent analyses as starting values.

The middle panels of Figure 2 show the spectra (black) of the mechanically aligned samples in the parallel orientation, while the lower panels are the spectra of the perpendicularly-orientated samples. The aligned EPR spectra clearly show the orientation dependent hyperfine splitting, where the hyperfine splitting is at a minimum (7.3 G for TOAC8 and 9.6 G for TOAC14) at the parallel orientation ( $n \parallel B_0$ ), and becomes maximum (29.3 G for TOAC8 and 30.0 G for TOAC14) at the perpendicular orientation ( $n \perp B_0$ ) [5]. This type of orientation dependent hyperfine splitting arises because the molecular axis i.e. the  $z$ -axis of the TOAC nitroxide lies nearly perpendicular to the static magnetic field ( $B_0$ ) when the glass plates are aligned parallel, which results in a minimal hyperfine splitting value. On the other hand, for the surface peptide magainin-2 used in this study, the nitroxide  $z$ -axis adopts the full range of orientations relative to  $B_0$  when glass plates are aligned perpendicular because the protein is oriented randomly with respect to the membrane surface ( $0 < \zeta < 360^\circ$ ). The resulting spectra show a broad range of hyperfine splittings.

The fits obtained from the non-linear least-squares analyses of the data from the singly-labeled aligned samples are shown in Figure 2 (red lines) and the best-fit parameters are given in Table 2. These fits were obtained by simultaneously fitting the two spectra for a given sample obtained at different sample alignments. A helix tilt angle,  $\nu$ , of  $81^\circ$  was assumed as reported in the previous study [5]. The best-fit angle between the nitroxide  $Z$ -axis and the helix axis,  $\theta$ , was determined to be  $43^\circ$  for TOAC8 and  $18^\circ$  for TOAC14 while modeling of the TOAC-labeled magainin peptides yielded the values of  $11^\circ$  for TOAC8 and  $13^\circ$  for TOAC14. The value of the angle  $\theta$  for TOAC14 agrees well with the experiment and modeling. The disagreement in the value of angle  $\theta$  for TOAC8 may be due to the fact that the  $N$ -terminus of the helix is interacting strongly with the surface of the membrane causing slight influence in the orientation of the nitroxide  $z$ -axis. Additional efforts were made to model these data assuming that there were two populations with different values for the angles  $\theta$  and  $\phi$ . These efforts did not result in significantly better fits. It is possible that at the relatively high temperatures employed (318 K), there is rapid intraconversion between two conformers of the TOAC ring. The values of  $\theta$  obtained in the current study favorably agree with the value of  $21^\circ$  previously reported for the twist boat conformer of the TOAC label [8]. The  $A$  and  $g$  tensor values for the aligned samples were found to be slightly deviated from the randomly dispersed samples to obtain better fit.

The EPR magnetic tensor ( $g$  and  $A$ ) anisotropies are sensitive to local polar environments, site specific molecular motion and temperature of the system [53–58]. The inspection of the root mean square deviation (RMSD) profiles (Figure S1) obtained from the molecular dynamics simulation of wild-type magainin-2 peptide in the presence of DMPC bilayers indicated that the residue at the 14<sup>th</sup> position is more mobile and flexible when compared to the residue at the 8<sup>th</sup> position. The deviation in the  $A$  and  $g$  parameters may arise due to the difference in local polarity and dielectric constants caused by a variation in lipid surface hydration level. The dynamic variation of residue sites in magainin-2 may have also contributed in the artifacts introduced in the experimental spectra of the aligned samples

causing discrepancies in the static magnetic parameters while obtaining the best fits of the experimental data.

Figure 3 shows the CW-EPR spectra of the dual TOAC-labeled magainin-2 peptide. The upper panel (A) shows the spectrum of the randomly-dispersed sample. Figures 3(B) and 3(C) reveal parallel-aligned, and the perpendicular-aligned spectra of doubly-labeled magainin-2 peptide in planar quartz-supported DMPC bilayers. Line broadening due to electron-electron dipolar interactions is clearly observed in all three spectra in comparison to the corresponding spectra of the singly-labeled peptides in Figure 2.

The fit overlaid on the randomly dispersed sample (Figure 3A) assumes a single distance and orientation between the two TOAC labels. The best-fit distance was obtained as  $R = 14.3 \text{ \AA}$ . There are a number of different sets of angles that are symmetry-related and give equivalent fits to the data. One such set of angles is given in Table 3a. Alternatively, a fit to this spectrum using a convolution approach which assumes an isotropic distribution in the relative orientation of the two angles (results not shown) gave a poor fit.

The parameters for the best global fit to the spectra of the parallel-aligned (Figure 3B) and the perpendicular-aligned samples (Figure 3C) are also given in Table 3b. The global fit was performed with the label at site 14 as a reference and the values of  $\psi_0$ ,  $\sigma_\psi$ ,  $\theta$ , and  $\phi$  were taken from the fit of the data in Figures 2E and 2F (Table 2). The best-fit inter-electron distance was found to be  $15.3 \text{ \AA}$ . Again, there are a number of sets of angles which are symmetry related and given equivalent fits to the data. For one such set of angles, the two angles defining the inter-electron vector are  $\xi = 64^\circ$  and  $\eta = 176^\circ$ . The Euler angles that orient TOAC8 nitroxide with respect to the TOAC14 (first nitroxide) are  $\alpha = 21^\circ$ ,  $\beta = 6^\circ$ , and  $\gamma = 295^\circ$ .

A number of factors influence the precision with which the various parameters defining the geometry between two dipolar-coupled labels can be determined [59]. In order to assess whether the global analysis of the spectra from aligned samples offers advantages over the analysis of a single spectrum from a randomly dispersed sample, confidence intervals were calculated for the various parameters. Representative confidence intervals for the Euler angles  $\alpha$ ,  $\beta$ , and  $\gamma$  are shown in Figure 4. From these plots, the uncertainty in a given parameter can be estimated from the range of values which fall below the horizontal dashed lines. These results demonstrate that the global analysis of the aligned data gives much more precise estimates of the angles  $\alpha$ ,  $\beta$ , and  $\gamma$  than that can be obtained from the analysis of the randomly dispersed data. The confidence intervals for the remaining angles  $\xi$  and  $\eta$ , and distance  $R$  are given in Figure S2 (see Supporting Information).

Given the conditions that were employed (i.e. temperature 318 K) we would not expect that we could get good fits to the data using rigid-limit tensors without explicitly including dynamics in the model used for the simulations. Explicitly including dynamics in the simulation model is beyond the scope of this work. Instead, given that the labeled peptides are in a membrane environment we would expect that the most significant motions of the labels are local rather than global. Our strategy is to assume that these local motions are



rapid and to fit the data using partially motionally-averaged tensors to account for these rapid local motions. We successfully used this strategy in the previous M26 paper.<sup>1</sup>

The tensor values for the two sites may be slightly different from each other. Small differences may be due to differences in polarity, dielectric or to differences in local dynamics. While we still would expect that we could fit the isotropic and aligned data with the same tensor values it is important to remember that the fits using partially motionally-averaged tensors are approximations. The local dynamics and thus the apparent best-fit tensor values would be somewhat different in isotropic versus aligned samples. Also, it is possible that there are significant differences in the local dynamics for the two samples. In any event, unlike for the M26<sup>1</sup> it is apparent just from looking at the spectra that the  $A_{zz}$  values are different for the aligned versus isotropic singly labeled samples. In order to justify the use of these altered tensor values, simulations of the aligned data using a fixed values of  $g$  and  $A$ -tensors obtained from the best fit unoriented singly labeled spectra were performed (see Figure S3). These fits are clearly not as good as those presented in Figure 2, however, the fit parameters obtained are similar ( $\theta = 30^\circ$  versus  $43^\circ$  and  $\phi = 210^\circ$  versus  $225^\circ$  for site 8, and  $\theta = 14^\circ$  versus  $18^\circ$  and  $\phi = 243^\circ$  versus  $235^\circ$  for site 14). This suggests that the use of altered tensor values in the simulation procedure didn't significantly influence the reported fit angles but greatly improved the quality of spectral fits. The isotropic values ( $(g_x + g_y + g_z)/3$ ) for all the samples are consistent.

The EPR membrane alignment is challenging for surface peptides especially doubly spin labeled peptides. Since the dynamics and fluctuations of different sites of the peptide are different, data analysis is also very complicated. This method of data analysis can be further extended to account for spin label dynamics, and include all the single and double labeled aligned data in a global fitting procedure to extract all the fitting parameters (distance/angles) simultaneously.

Molecular modeling studies on the magainin-2 peptide were conducted using MolMol and Visual molecular dynamics programs (see Material and Method section for details). The various parameters that define the geometry and distance of the two TOAC spin probes in magainin-2 peptides were calculated. The distance between two TOAC nitroxides and their orientation angles obtained from the spectral simulations were found comparable with the molecular modeling studies. Using the coordinates of the nitroxide nitrogen and oxygen atoms in a dual-labeled magainin-2 peptide, we calculated an internitroxide distance of 13.3 Å, which is close to the 15.3 Å distance obtained from the aligned CW-EPR spectra simulations. The rotational Euler angles that define the relative orientation of TOAC14 nitroxide with respect to TOAC8 nitroxide also agreed well (except the third angle)  $\alpha = 21^\circ$ ,  $\beta = 6^\circ$ , and  $\gamma = 295^\circ$  with EPR spectral simulations and  $\alpha = 27^\circ$ ,  $\beta = 12^\circ$ , and  $\gamma = 212^\circ$  from modeling studies.

In order to directly compare the results from fitting the aligned EPR spectra to those from the modeling studies, a set of  $x$ -,  $y$ -, and  $z$ -axes were calculated from the distance and angles given in Table 3b and overlaid on the model peptide. The results are shown in three different views in Figure 5.

## Conclusion

The internitroxide distance and relative orientation of two TOAC nitroxides of dual TOAC-labeled magainin-2 peptide have been successfully determined by orienting dual TOAC-labeled magainin-2 peptide in mechanically aligned glass plates, applying rigorous spectral simulation techniques, and simultaneously analyzing data at two sample orientations (0° and 90°). This is an important technique as samples are easy to prepare and the system provides adequate lipid hydration maintaining the rigidity of the nitroxide side chain leading to more accurate distance and orientation measurements. Distance measurements can be performed at conventional X-band (~9 GHz) EPR room temperature or even higher (i.e. 318K) and sample orientations can be adjusted from 0° to 90° or any angles in between to get detailed structural parameters needed for distance measurements.

## Supplementary Material

Refer to Web version on PubMed Central for supplementary material.

## Acknowledgements

This project was supported by NIGMS/NIH (GM108026), NSF (CHE-1305664), and MRI-0722403 to GAL and NIHGM080513 to E.J.H.

## References

1. Ghimire H, Hustedt EJ, Sahu ID, Inbaraj JJ, McCarrick R, Mayo DJ, Benedikt MR, Lee RT, Grosser SM, Lorigan GA. Distance Measurements on a Dual-Labeled TOAC AChR M28 Peptide in Mechanically Aligned DMPC Bilayers via Dipolar Broadening CW-EPR Spectroscopy. *J. Phys. Chem. B.* 2012; 116:3866–3873. [PubMed: 22379959]
2. Hubbell WL, Altenbach C. Investigation of structure and dynamics in membrane-proteins using site-directed spin labeling. *Curr. Opin. Struct. Biol.* 1994; 4:566–573.
3. Fanucci GE, Cafiso DS. Recent advances and applications of site-directed spin labeling. *Curr. Opin. Struct. Biol.* 2006; 16:644–653.
4. Klug CS, Feix JB. Methods and Applications of Site-Directed Spin Labeling EPR Spectroscopy. *Methods Cell Biol.* 2008; 84:617–658. [PubMed: 17964945]
5. Mayo DJ, Inbaraj JJ, Subbaraman N, Grosser SM, Chan CA, Lorigan GA. Comparing the Structural Topology of Integral and Peripheral Membrane Proteins Utilizing Electron Paramagnetic Resonance Spectroscopy. *J. Am. Chem. Soc.* 2008; 130:9656–9657. [PubMed: 18598031]
6. Sahu ID, McCarrick RM, Lorigan GA. Use of Electron Paramagnetic Resonance to Solve Biochemical Problems. *Biochemistry.* 2013; 52:5967–5984. [PubMed: 23961941]
7. Sahu ID, McCarrick RM, Troxel KR, Zhang R, Smith JH, Dunagan MM, Swartz MS, Rajan PV, Kroncke BM, Sanders CR, Lorigan GA. DEER EPR measurement for Membrane Protein Structures via Bifunctional Spin Labels and Lipodisq Nanoparticles. *Biochemistry.* 2013; 52:6627–6632. [PubMed: 23984855]
8. Hanson P, Anderson DJ, Martinez G, Millhauser G, Formaggio F, Crisma M, Toniolo C, Vita C. Electron spin resonance and structural analysis of water soluble, alanine-rich peptides incorporating TOAC. *Mol. Phys.* 1998; 95:957–966.
9. Hustedt EJ, Smirnov AI, Laub CF, Cobb CE, Beth AH. Molecular distances from dipolar coupled spin-labels: The global analysis of multifrequency continuous wave electron paramagnetic resonance data. *Biophys. J.* 1997; 72:1861–1877. [PubMed: 9083690]
10. Steinhoff HJ, Radzwill N, Thevis W, Lenz V, Brandenburg D, Antson A, Dodson G, Wollmer A. Determination of interspin distances between spin labels attached to insulin: Comparison of

- electron paramagnetic resonance data with the x-ray structure. *Biophys. J.* 1997; 73:3287–3298. [PubMed: 9414239]
11. Jeschke G, Koch A, Jonas U, Godt A. Direct conversion of EPR dipolar time evolution data to distance distributions. *J. Magn. Reson.* 2002; 155:72–82. [PubMed: 11945035]
  12. Borbat PP, Mchaourab HS, Freed JH. Protein structure determination using long-distance constraints from double-quantum coherence ESR: Study of T4 lysozyme. *J. Am. Chem. Soc.* 2002; 124:5304–5314. [PubMed: 11996571]
  13. Cai Q, Kusnetzow AK, Hubbell WL, Haworth IS, Gacho GPC, Van Eps N, Hideg K, Chambers EJ, Qin PZ. Site-directed spin labeling measurements of nanometer distances in nucleic acids using a sequence-independent nitroxide probe. *Nucleic Acids Research.* 2006; 34:4722–4730. [PubMed: 16966338]
  14. Sen KI, Logan TM, Fajer PG. Protein dynamics and monomer-monomer interactions in AntR activation by electron paramagnetic resonance and double electron-electron resonance. *Biochemistry.* 2007; 46:11639–11649. [PubMed: 17880108]
  15. Schiemann O, Prisner TF. Long-range distance determinations in biomacromolecules by EPR spectroscopy. *Quarterly Rev. Biophys.* 2007; 40:1–53.
  16. Ghimire H, McCarrick RM, Budil DE, Lorigan GA. Significantly Improved Sensitivity of Q-Band PELDOR/DEER Experiments Relative to X-Band Is Observed in Measuring the Intercoil Distance of a Leucine Zipper Motif Peptide (GCN4-LZ). *Biochemistry.* 2009; 48:5782–5784. [PubMed: 19476379]
  17. Rabenstein MD, Shin YK. Determination of the distance between 2 spin labels attached to a macromolecule. *Proc. Natl. Acad. Sci. U.S.A.* 1995; 92:8239–8243. [PubMed: 7667275]
  18. Altenbach C, Oh KJ, Trabanino RJ, Hideg K, Hubbell WL. Estimation of inter-residue distances in spin labeled proteins at physiological temperatures: Experimental strategies and practical limitations. *Biochemistry.* 2001; 40:15471–15482. [PubMed: 11747422]
  19. Mchaourab HS, Oh KJ, Fang CJ, Hubbell WL. Conformation of T4 lysozyme in solution. Hinge-bending motion and the substrate-induced conformational transition studied by site-directed spin labeling. *Biochemistry.* 1997; 36:307–316. [PubMed: 9003182]
  20. Hustedt EJ, Stein RA, Sethaphong L, Brandon S, Zhou Z, DeSensi SC. Dipolar coupling between nitroxide spin labels: The development and application of a tether-in-acone model. *Biophys. J.* 2006; 90:340–356. [PubMed: 16214868]
  21. Hustedt EJ, Beth AH. Nitroxide spin-spin interactions: Applications to protein structure and dynamics. *Annu. Rev. Biophys. Biomol. Struct.* 1999; 28:129–153. [PubMed: 10410798]
  22. Opella SJ, Marassi FM. Structure determination of membrane proteins by NMR spectroscopy. *Chemical Reviews.* 2004; 104:3587–3606. [PubMed: 15303829]
  23. Opella SJ. NMR and membrane proteins. *Nature Struct. Biol.* 1997; 4:845–848. [PubMed: 9377156]
  24. Bechinger B, Zasloff M, Opella SJ. Structure and orientation of the antibiotic peptide magainin in membranes by solid-state nuclear magnetic resonance spectroscopy. *Protein Science.* 1993; 2:2077–2084. [PubMed: 8298457]
  25. Ramamoorthy A, Marassi FM, Zasloff M, Opella SJ. 3-Dimensional Solid-State Nmr-Spectroscopy of a Peptide Oriented in Membrane Bilayers. *J. Biomol. NMR.* 1995; 6:329–334. [PubMed: 8520224]
  26. Bechinger B, Kim Y, Chirlian LE, Gesell J, Neumann JM, Montal M, Tomich J, Zaslof M, Opella SJ. Orientations of Amphipathic Helical Peptides in Membrane Bilayers Determined by Solid-State NMR Spectroscopy. *J. Biomol. NMR.* 1991; 1:167–174. [PubMed: 1726781]
  27. Sato H, Felix JB. Peptide-membrane interactions and mechanisms of membrane destruction by amphipathic alpha-helical antimicrobial peptides. *Biochim. Biophys. Acta-Biomembranes.* 2006; 1758:1245–1256.
  28. Papo N, Shai Y. Host defense peptides as new weapons in cancer treatment. *Cellular and Molecular Life Sciences.* 2005; 62:784–790. [PubMed: 15868403]
  29. Hoskin DW, Ramamoorthy A. Studies on anticancer activities of antimicrobial peptides. *Biochim. Biophys. Acta.* 2008; 1778:357–375. [PubMed: 18078805]

30. Ramos R, Moreira S, Rodrigues A, Gama M, Domingues L. Recombinant expression and purification of the antimicrobial peptide magainin-2. *Biotechnology Progress*. 2013; 29:17–22. [PubMed: 23125137]
31. Westerhoff HV, Juretic D, Hendler RW, Zasloff M. Magainins and the disruption of membrane-linked free-energy transduction. *Proc. Natl. Acad. Sci. U. S. A.* 1989; 86:6597–6601. [PubMed: 2671997]
32. Cruciani RA, Barker JL, Zasloff M, Chen HC, Colamonici O. Antibiotic Magainins Exert Cytolytic Activity Against Transformed-Cell Lines Through Channel Formation. *Proc. Natl. Acad. Sci. U. S. A.* 1991; 88:3792–3796. [PubMed: 1708887]
33. Gallucci E, Meleleo D, Micelli S, Picciarelli V. Magainin 2 channel formation in planar lipid membranes: the role of lipid polar groups and ergosterol. *Europ. Biophys. J. Biophys. Lett.* 2003; 32:22–32.
34. Gesell J, Zasloff M, Opella SJ. Two-dimensional H-1 NMR experiments show that the 23-residue magainin antibiotic peptide is an alpha-helix in dodecylphosphocholine micelles, sodium dodecylsulfate micelles, and trifluoroethanol/water solution. *J. Biomol. NMR.* 1997; 9:127–135. [PubMed: 9090128]
35. Marchetto R, Schreier S, Nakaie CR. A Novel Spin-Labeled Amino-Acid Derivative For Use in Peptide-Synthesis - (9-Fluorenylmethyloxycarbonyl)-2,2,6,6-Tetramethylpiperidine-N-Oxyl-4-Amino-4-Carboxylic Acid. *J. Am. Chem. Soc.* 1993; 115:11042–11043.
36. Victor, KG. An Investigation of the Electrochemical Interactions Between Acidic Phospholipid Membranes and Charged Peptides Using Electron Paramagnetic Resonance. University of Virginia; 2000.
37. Martin L, Ivancich A, Vita C, Formaggio F, Toniolo C. Solid-phase synthesis of peptides containing the spin-labeled 2,2,6,6-tetramethylpiperidine-1-oxyl-4-amino-4-carboxylic acid (TOAC). *J. Pept. Res.* 2001; 58:424–432. [PubMed: 11892851]
38. Inbaraj JJ, Cardon TB, Laryukhin M, Grosser SM, Lorigan GA. Determining the topology of integral membrane peptides using EPR spectroscopy. *J. Am. Chem. Soc.* 2006; 128:9549–9554. [PubMed: 16848493]
39. Karim CB, Zhang Z, Thomas DD. Synthesis of TOAC spin-labeled proteins and reconstitution in lipid membranes. *Nature Protocols.* 2007; 2:42–49. [PubMed: 17401337]
40. Carpino LA. 1-Hydroxy-7-Azabenzotriazole - an Efficient Peptide Coupling Additive. *J. Am. Chem. Soc.* 1993; 115:4397–4398.
41. Carpino LA, Elfaham A, Minor CA, Albericio F. Advantageous Applications of Azabenzotriazole (Triazolopyridine)-Based Coupling Reagents to Solid-Phase Peptide-Synthesis. *J. Chem. Soc., Chem. Commun.* 1994:201–203.
42. Inbaraj JJ, Laryukhin M, Lorigan GA. Determining the helical tilt angle of a transmembrane helix in mechanically aligned lipid bilayers using EPR spectroscopy. *J. Am. Chem. Soc.* 2007; 129:7710–7711. [PubMed: 17539638]
43. Opella SJ, Marassi FM, Gesell JJ, Valente AP, Kim Y, Oblatt-Montal M, Montal M. Structures of the M2 channel-lining segments from nicotinic acetylcholine and NMDA receptors by NMR spectroscopy. *Nat. Struct. Biol.* 1999; 6:374–379. [PubMed: 10201407]
44. Hustedt EJ, Cobb CE, Beth AH, Beechem JM. Measurement of Rotational-Dynamics by the Simultaneous Nonlinear-Analysis of Optical and EPR Data. *Biophys. J.* 1993; 64:614–621. [PubMed: 7682452]
45. Koradi R, Billeter M, Wuthrich K. MOLMOL: A program for display and analysis of macromolecular structures. *J. Mol. Graphics.* 1996; 14:51–55.
46. Humphrey W, Dalke A, Schulten K. VMD-Visual Molecular Dynamics. *J. Mol. Graphics.* 1996; 14:33–38.
47. Champaign, IL: Wolfram Research Inc.; Mathematica.
48. Phillips JC, Braun R, Wang W, Gumbart J, Tajkhorshid E, Villa E, Chipot C, Skeel RD, Kalé L, Schulten K. Scalable molecular dynamics with NAMD. *J. Comput. Chem.* 2005; 26:1781–1802. [PubMed: 16222654]
49. MacKerell AD, Bashford D, Bellott M, Dunbrack RL, Evanseck JD, Field MJ, Fischer S, Gao J, Guo H, Ha S, Joseph-McCarthy D, Kuchnir L, Kuczera K, Lau FTK, Mattos C, Michnick S, Ngo

- T, Nguyen DT, Prodhom B, Reiher WE, Roux B, Schlenkrich M, Smith JC, Stote R, Straub J, Watanabe M, Wiorcikiewicz-Kuczera J, Yin D, Karplus M. All-atom empirical potential for molecular modeling and dynamics studies of proteins. *J. Phys. Chem. B.* 1998; 102:3586–3616. [PubMed: 24889800]
50. MacKerell AD, Feig M, Brooks CL. Improved treatment of the protein backbone in empirical force fields. *J. Am. Chem. Soc.* 2004; 126:698–699. [PubMed: 14733527]
51. Jo S, Kim T, Iyer VG, Im W. Software news and updates - CHARNIM-GUI: A web-based graphical user interface for CHARMM. *J. Comput. Chem.* 2008; 29:1859–1865. [PubMed: 18351591]
52. Ramelot TA, Yang Y, Sahu ID, Lee H-W, Xiao R, Lorigan GA, Montelione GT, Kennedy MA. NMR structure and MD simulations of the AAA protease intermembrane space domain indicates peripheral membrane localization within the hexaoligomer. *Febs Letters.* 2013; 587:3522–3528. [PubMed: 24055473]
53. Finiguerra MG, Blok H, Ubbink M, Huber M. High-field (275 GHz) spin-label EPR for high-resolution polarity determination in proteins. *J. Magn. Reson.* 2006; 180:197–202. [PubMed: 16545591]
54. Fajer, PG. Electron Spin Resonance Labeling in Peptide and Protein Analysis. In: Meyers, RA., editor. *Encyclopedia of Analytical Chemistry.* New York: John Wiley & Sons Ltd.; 2000. p. 5725-5761.
55. Savitsky A, Mobius K. High-field EPR. *Photosynthesis Research.* 2009; 102:311–333. [PubMed: 19468856]
56. Mobius K, Schnegg A, Plato M, Fuchs MR, Savitsky A. High-field EPR spectroscopy on transfer proteins in biological action. *Acta Physica Polonica A.* 2005; 108:215–234.
57. Gaffney BJ, Marsh D. High-frequency, spin-label EPR of nonaxial lipid ordering and motion in cholesterol-containing membranes. *Proc. Natl. Acad. Sci. U. S. A.* 1998; 95:12940–12943. [PubMed: 9789019]
58. Savitsky A, Plato M, Moebius K. The Temperature Dependence of Nitroxide Spin-Label Interaction Parameters: a High-Field EPR Study of Intramolecular Motional Contributions. *Appl. Magn. Reson.* 2010; 37:415–434.
59. Hustedt, EJ., Beth, AH. Structural Information from CW-EPR Spectra of Dipolar Coupled Nitroxide Spin Labels. In: Berlinger, LJ, Eaton, SS., Eaton, GR., editors. *Biological Magnetic Resonance.* New York: Kluwer Academic/Plenum Publishers; 2000. p. 155-184.

**Highlights**

- 1) An EPR membrane alignment technique is applied to membrane peripheral protein
- 2) Distance and relative orientations were measured on peripheral membrane peptide
- 3) Aligned membrane protein samples provide better structure data than random samples

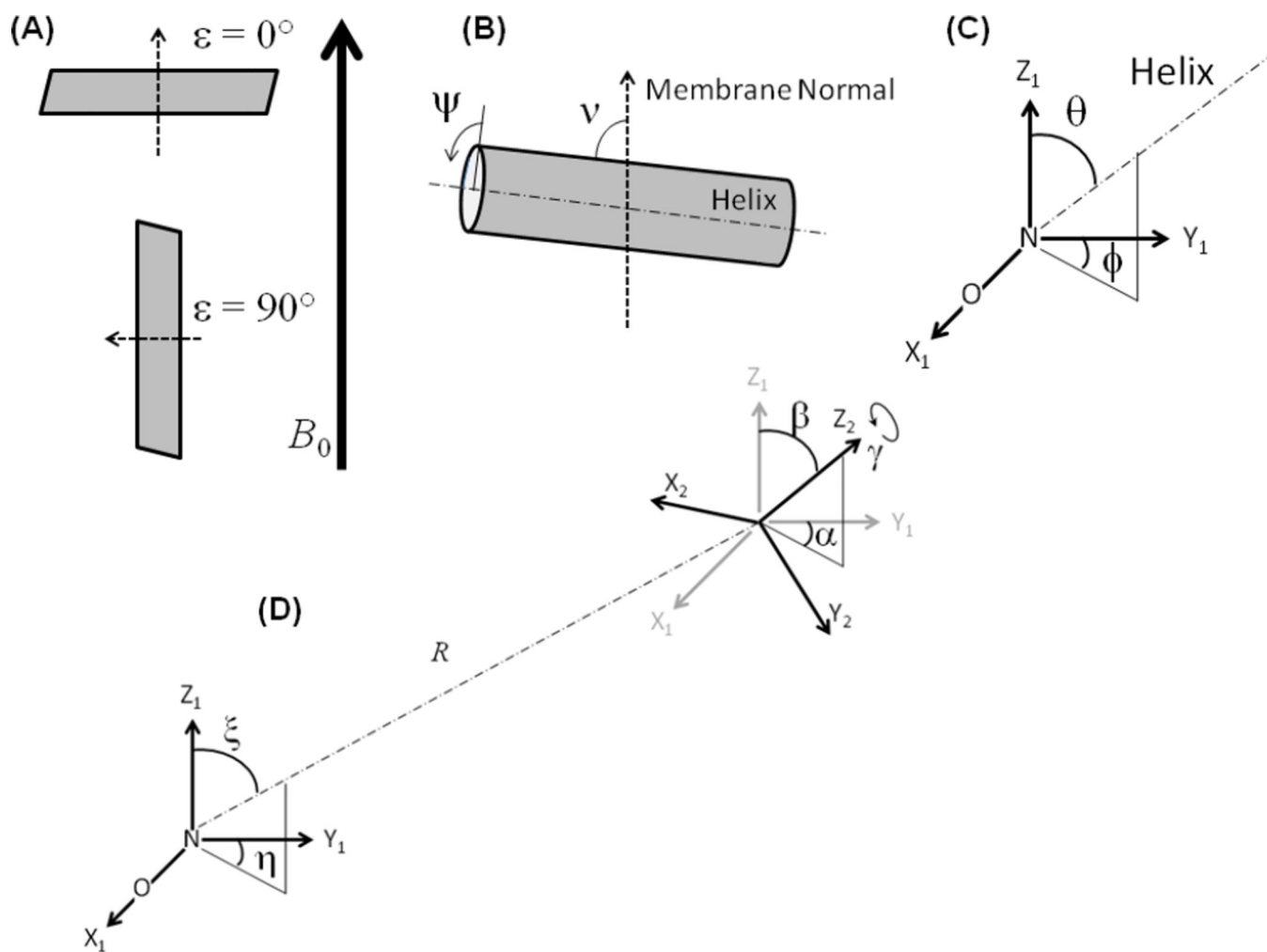


**Figure 1.**

Angles used in this study. (A) Two different sample orientations (parallel ( $\varepsilon=0^\circ$ ) and perpendicular ( $\varepsilon=90^\circ$ )) with respect to magnetic field ( $B_0$ ), (B) Helix tilt angle ( $\nu$ ) and rotational angle of peptide about the helix axis ( $\psi$ ), (C) Orientations of nitroxide with respect to helix axis ( $\theta$  and  $\phi$ ), and (D) Three Euler angles of rotation ( $\alpha$ ,  $\beta$  and  $\gamma$ ) and orientations ( $\eta$  and  $\xi$ ) of interelectron distance ( $R$ ) with respect to nitroxide position.

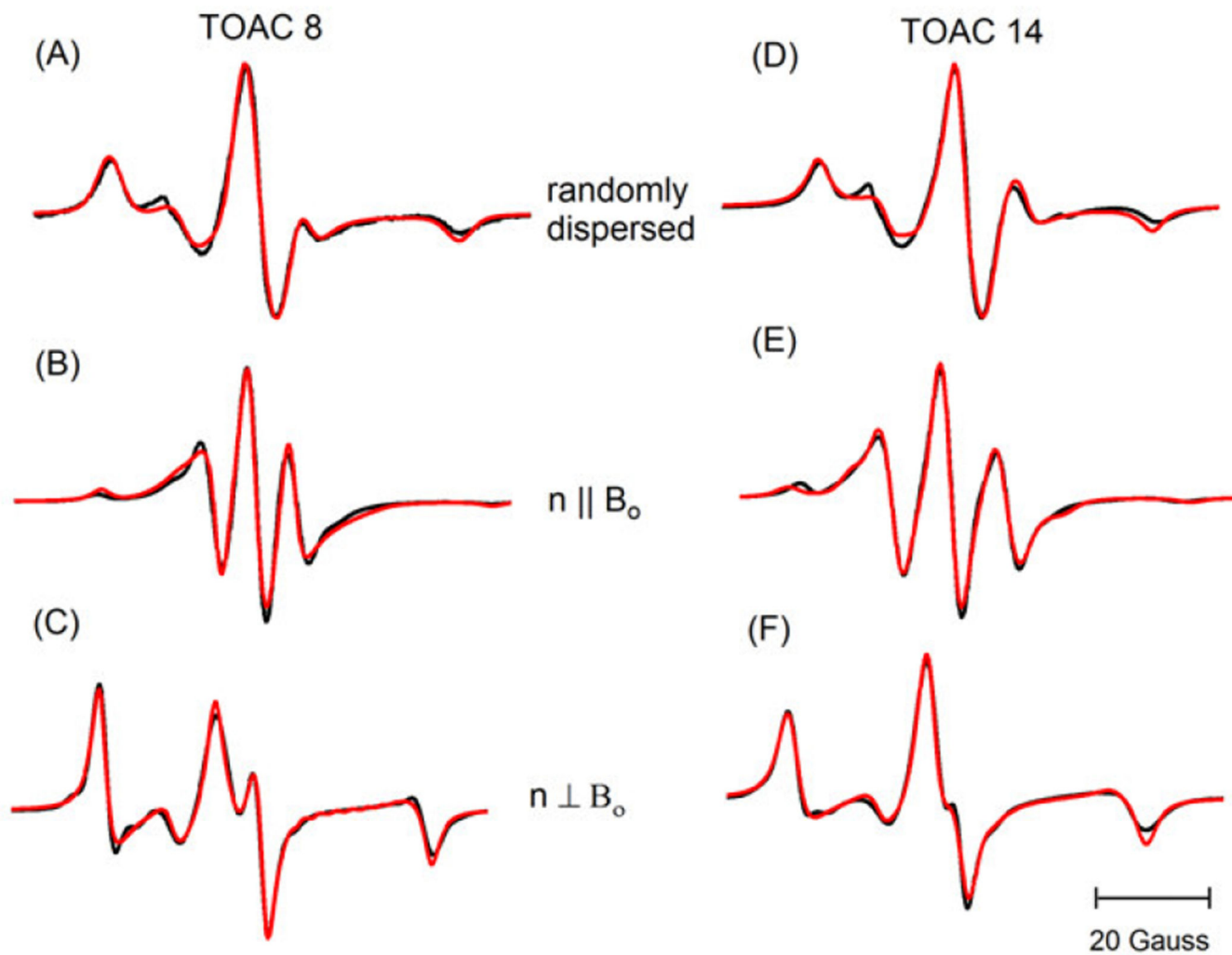


**Figure 2.** CW-EPR spectra (black lines) of TOAC8 (left) and TOAC14 (right) magainin- 2 peptides in DMPC bilayers at 318 K together with the best-fit simulations (red lines). The upper panels (A) and (D) contain spectra of randomly dispersed samples. The middle panels (B) and (E) contain spectra from parallel-aligned samples. The lower panels (C) and (F) contain spectra from the perpendicular-aligned samples. For each site, the  $n \parallel B_0$  and  $n \perp B_0$  were simultaneously analyzed to determine the best fit values of  $\psi_0$ ,  $\sigma_\psi$ ,  $\theta$ ,  $\phi$ , components of A and g tensors (Table 2). n represents the membrane normal.



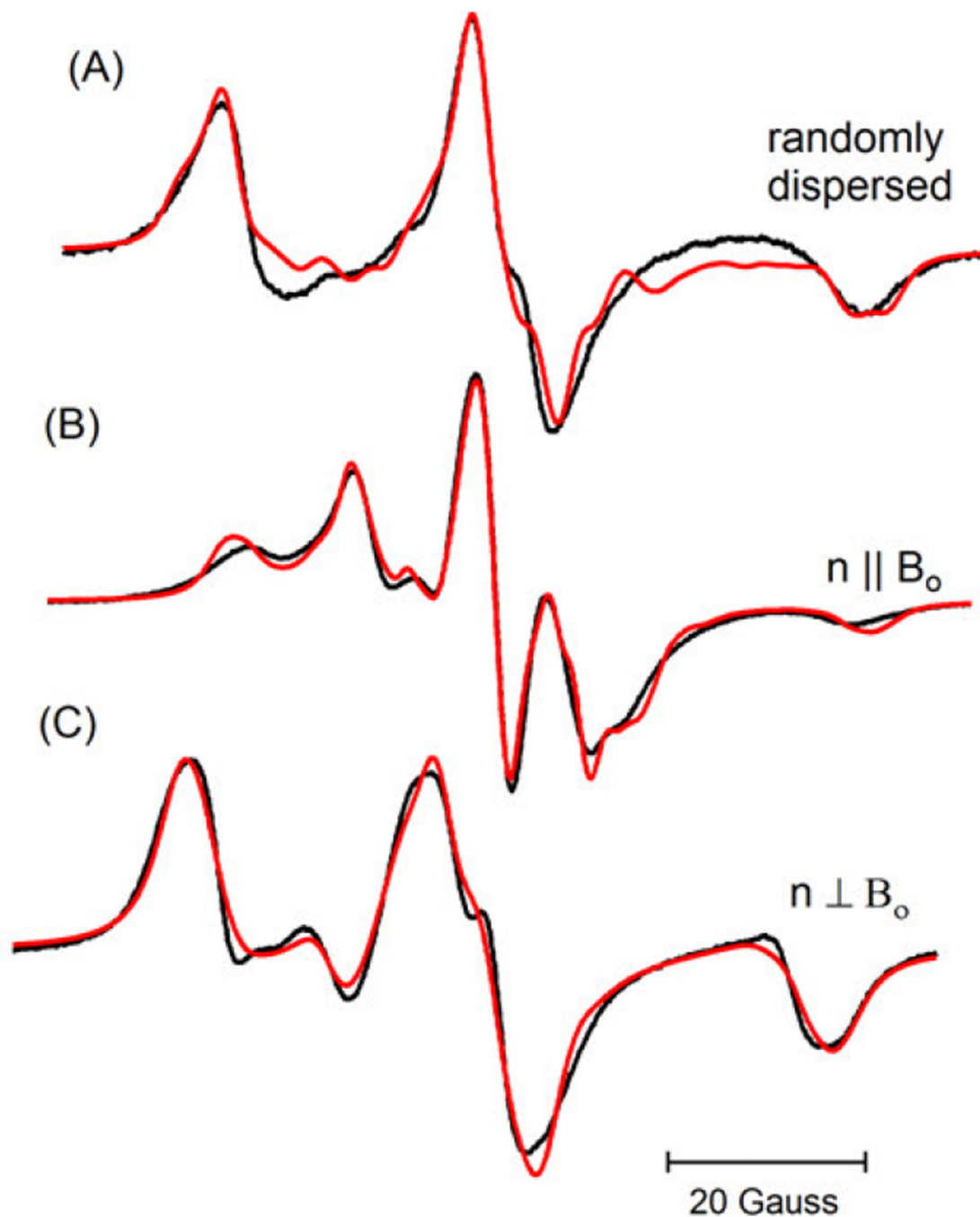


**Figure 3.** CW-EPR spectra for the doubly labeled magainin-2 peptide in DMPC bilayers at 318 K for the randomly-dispersed sample (A),  $n \parallel B_0$  sample (B), and  $n \perp B_0$  sample (C). The black lines represent experimental data and the red lines represent the best fit simulations. The  $n \parallel B_0$  and  $n \perp B_0$  data were simultaneously analyzed to determine the best fit values of  $\alpha$ ,  $\beta$ ,  $\gamma$ ,  $\xi$ ,  $\eta$ , and  $R$  (Table 3). A similar analysis was performed on the randomly-dispersed spectrum (Table 3).

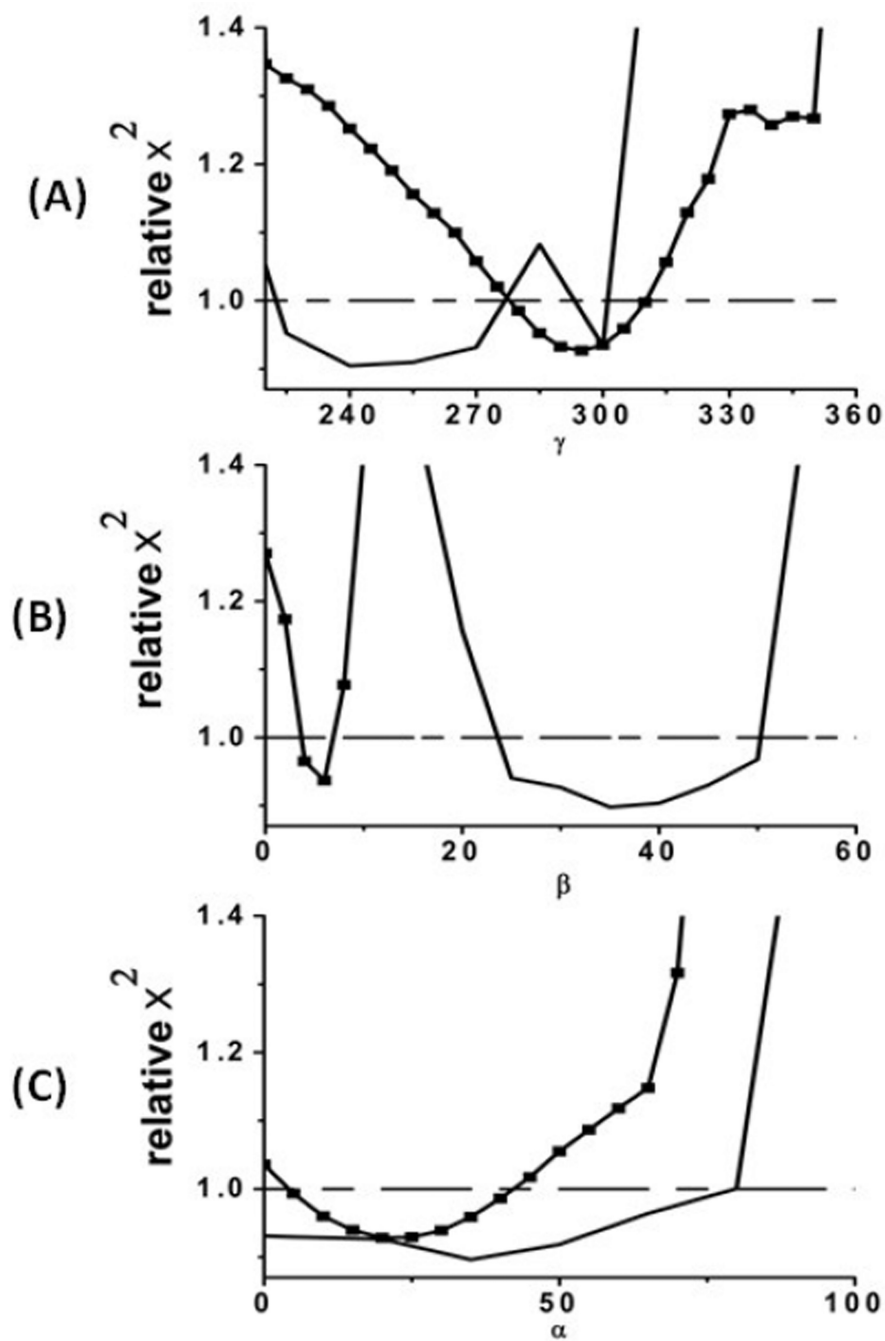


**Figure 4.** Confidence intervals for the angles  $\gamma$  (A),  $\beta$  (B), and  $\alpha$  (C). The best-fit  $\chi^2$  values obtained from fitting the two oriented spectra (black solid squares) and the isotropic spectrum (black solid line) are plotted for a linear sequence of values for the particular angle. The horizontal dashed lines are drawn at the  $\chi^2$  value corresponding to an approximate 95% confidence level calculated using the F-statistic.

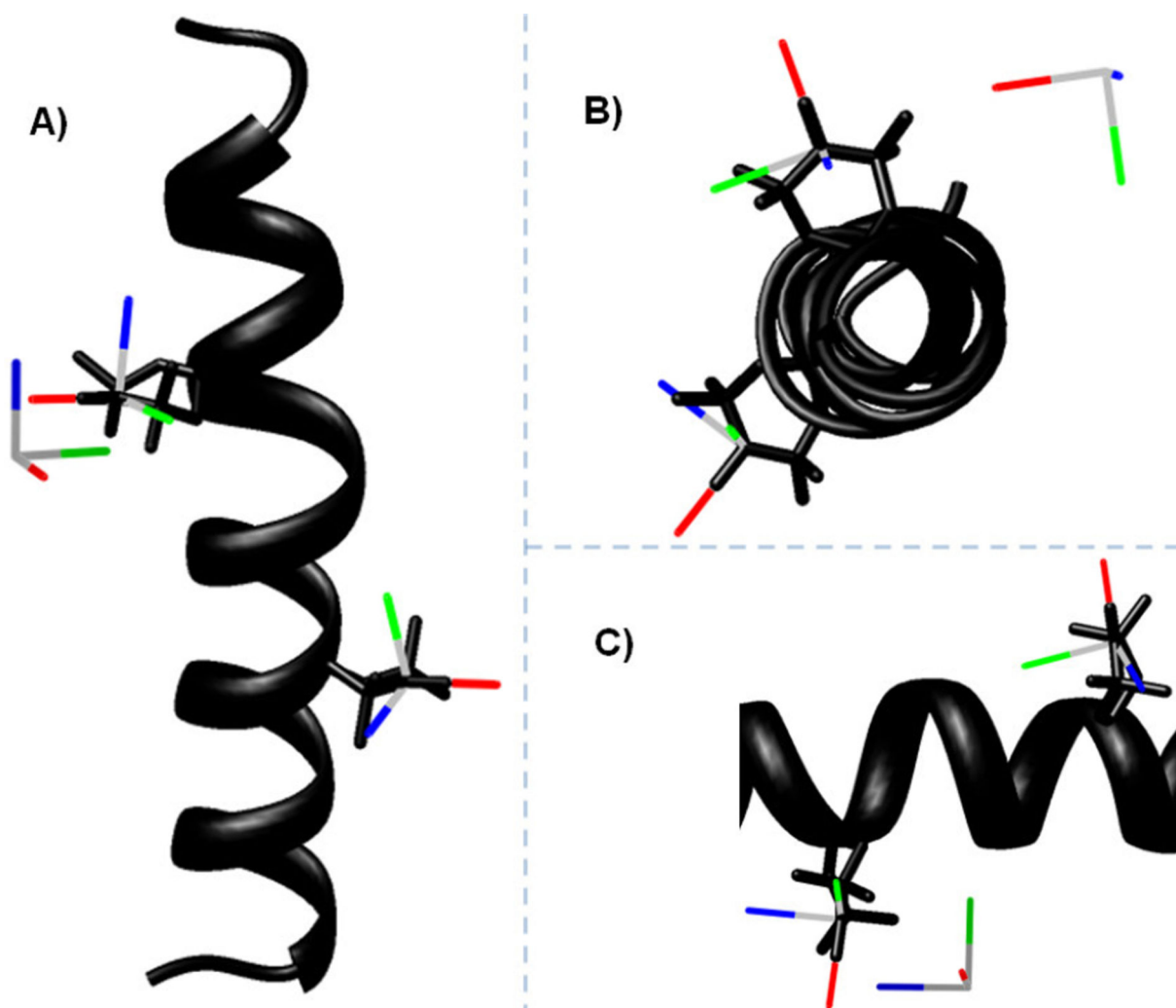


**Figure 5.** Three different views comparing the best-fit results to the predicted model of the doubly-labeled peptide. For the predicted model, the helix is shown in black. The nitrogen, oxygen, and adjacent carbon atoms of the TOAC nitroxides are shown as stick models. The TOACs at residues 8 and 14 are colored in black. Overlaid on the TOAC for the model are the calculated x-, y-, and z-axes of the TOAC nitroxides in red, green, and blue respectively. The set of additional axes represent the position and orientation of TOAC8 relative to TOAC14 as back calculated for the best-fit values of the distance and angles determined in Figure 3. Three different views are shown each rotated by 90°.

**Table 1**

Parameters for the best-fit simulation of randomly-dispersed singly-labeled magainin-2 peptides. The  $lw_1$  represents Lorentzian linewidth (full width at half maximum (FWHM)) and  $lw_G$  represents Gaussian linewidth (FWHM).

site	$g_{xx}$	$g_{yy}$	$g_{zz}$	$A_{xx}$ (G)	$A_{yy}$ (G)	$A_{zz}$ (G)	$lw_1$ (G)	$lw_G$ (G)
8	2.0073	2.0060	2.0032	10.3	5.7	29.7	1.3	1.6
14	2.0067	2.0061	2.0037	12	7.5	28.4	1.9	1.0

Parameters for the best-fit simulation of aligned singly-labeled magainin-2 peptides compared to the parameters from molecular modeling. The  $lw_1$  represents Lorentzian linewidth (FWHM).

**Table 2**

	site	$g_{xx}$	$g_{yy}$	$g_{zz}$	$A_{xx}$ (G)	$A_{yy}$ (G)	$A_{zz}$ (G)	$lw_1$ (G)	$\psi_0$	$\sigma_\psi$	$\theta$	$\phi$	isotropic fraction
Fit	8	2.0083	2.0058	2.0024	8.1	5.0	31.2	1.9	76°	20°	43°	225°	0.26
Model	8	-	-	-	-	-	-	-	-	-	11°	277°	-
Fit	14	2.0070	2.0067	2.0029	4.1	9.7	32.1	2.4	86°	47°	18°	235°	0.29
Model	14	-	-	-	-	-	-	-	-	-	13°	159°	-

Parameters for the best-fit simulation of doubly-labeled magainin-2 peptides for both the randomly-dispersed and aligned samples compared to the parameters from molecular modeling. The  $lw_1$  represents Lorentzian linewidth (FWHM).

**Table 3**

	$\gamma$	$\beta$	$\alpha$	$\xi$	$\eta$	$R$ (Å)	$lw_1$ (G)	isotropic fraction
<b>a</b>	isotropic 246°	37°	36°	62°	105°	14.3	1.1	1.00
<b>b</b>	aligned 295°	6°	21°	64°	176°	15.3	2.8	0.5
<b>c</b>	model 212°	12°	27°	40°	210°	13.3	-	-